



Deposited via The University of Sheffield.

White Rose Research Online URL for this paper:

<https://eprints.whiterose.ac.uk/id/eprint/220939/>

Version: Accepted Version

Proceedings Paper:

Whittaker, M., Limbu, A., Pope, D. et al. (2023) Development of a predictive framework for assessing the viability and power of ideal and non-ideal explosives with respect to mitigating and protecting against energetic effects. In: Proceedings of the 26th International Symposium on Military Aspects of Blast and Shock (MABS26). 26th International Symposium on Military Aspects of Blast and Shock (MABS26), 04-08 Dec 2023, Wollongong, Australia. Military Aspects of Blast and Shock (MABS).

© 2023 MABS 26. For reuse permissions, please contact the Author(s).

Reuse

Items deposited in White Rose Research Online are protected by copyright, with all rights reserved unless indicated otherwise. They may be downloaded and/or printed for private study, or other acts as permitted by national copyright laws. The publisher or other rights holders may allow further reproduction and re-use of the full text version. This is indicated by the licence information on the White Rose Research Online record for the item.

Takedown

If you consider content in White Rose Research Online to be in breach of UK law, please notify us by emailing eprints@whiterose.ac.uk including the URL of the record and the reason for the withdrawal request.

DEVELOPMENT OF A PREDICTIVE FRAMEWORK FOR ASSESSING THE VIABILITY AND POWER OF IDEAL AND NON-IDEAL EXPLOSIVES WITH RESPECT TO MITIGATING AND PROTECTING AGAINST ENERGETIC EFFECTS

M.J. Whittaker¹, A. Limbu¹, D.J. Pope¹, A. Tyas², T. Lodge² & D. Farrimond²

¹ *Physical Sciences Group, Platform Systems Division, Dstl Porton Down, Salisbury, Wiltshire SP4 0JQ, United Kingdom*

² *Blastech Ltd, 40 Leavygreave Road, Sheffield, S3 7RD, UK*

&

*Department of Civil and Structural Engineering, University of Sheffield
Mappin Street, Sheffield, S1 3JD, UK*

Key words: Non-ideal explosives, Modelling, Experiments, Energetics, APOLLO

ABSTRACT

Within the UK Defence and Security domain numerical modelling is being increasingly used to rapidly assess the viability and power of a broad range of both ideal and non-ideal explosive materials. This work allows analysts and engineers to develop mitigating and protective solutions in the case of potential conventional or terrorist attack. Considering the broad scope of available explosives, a combination of highly efficient analytical and experimental techniques have been developed by Dstl, and its research partners, to accurately parameterise explosive materials for simulating initiation, energetic expansion and secondary combustion events. This paper describes how precision experimentation (including cylinder expansion testing), combined with thermochemical analysis, serve as a foundation within this process. With reference to very near-field experimental validation data it also provides Dstl's experience concerning the predictive accuracy of various hydrocode-based modelling approaches, with particular emphasis on appropriately handling the difference between ideal and non-ideal explosive behaviour.

INTRODUCTION

The experimental determination of parameters and development of methodologies for characterising the effects of energetic materials are well established, however, several significant issues with current approaches still exist. As well as being a generally expensive process, the generation of near-field blast data, for example, requires highly specialist facilities and dedicated expertise while the parameterisation of non-ideal materials at large mass ranges may be required for testing.

Therefore, in recent years, significant effort has been made by Dstl, and its research partners, to develop numerical methodologies to capture such phenomena. In addition, focus has been placed

Non-ideal energetic materials can have large critical diameter and run to detonation distances. Due to this ¹ behaviour materials can need to be tested at large masses (e.g. 100kg+) to experience their "ideal" behaviour, where smaller-scale tests also need to be conducted to characterise and validate their mass scaling behaviour

on generating thermochemical methods for parameter determination and the development of suitable experimental methods to validate these approaches.

With these objectives in mind, extensive, well-controlled tests have been conducted on a range of materials to both understand behaviour and provide data for analysis. These include PE4, PE8, PE10, PBXN-109, PBXN-111 and ANFO (Ammonium Nitrate Fuel Oil).

International collaboration has played a large part in the energetics modelling capability at Dstl, including:

- Test series conducted by CEA (The French Alternative Energies and Atomic Energy Commission), France
- Numerical functionality development by AFRL (Air Force Research Laboratory), US
- Development and functionality implementation for APOLLO Blastsimulator by Fraunhofer EMI (Ernst Mach Institut)
- Code access, such as CTH developed by SANDIA, US

A range of software tools has been used in this study, for the validation, verification and benchmarking of energetic materials, including:

- APOLLO, Autodyn and CTH for Eulerian simulations of energetic materials
- Cheetah and EXPLO5 thermochemical codes for the development of EOS parameters to describe the behaviour of energetic materials within the above physics software
- Conwep for providing analytical predictions for comparison to physics modelling results, as a sanity check

EXPERIMENTAL DEVELOPMENT

In order to provide validation data for numerical simulations, four test setups have been generally used associated with the following regimes and configurations:

- Near-field – scaled distance $<1 \text{ m/kg}^{1/3}$
- Far-field – scaled distance $2 < Z < 12 \text{ m/kg}^{1/3}$
- Confined
- CYLEX (CYLinder EXpansion)

Understanding the mechanisms and magnitudes of blast loading on targets from near-field detonations of high explosive charges is of key importance for the analysis and design of protective structures. However, there is relatively little definitive experimental data on the measurement of these loads and consequently the numerical predictions of near-field blast loading are largely unvalidated.

The issue for experimentalists is that measurement devices must be able to record very high pressures ($>>10^6 \text{ Pa}$) with microsecond-scale temporal resolution in environments where the high temperature explosive fireball will directly interact with the sensors. Whilst conventional piezo-electric and piezo-resistive pressure sensors have the range and bandwidth to make these measurements, they are prone to damage in these aggressive environments. Over 100 years ago, Bertram Hopkinson developed the use of the pressure bar which was to bear his name in order to

measure the loading from projectile impact and contact loading from detonators [1]. The original Hopkinson Pressure Bar (HPB) comprised a long, thin cylindrical bar acting as a waveguide for the stress pulse generated by the loading, with the impulse contained in the stress pulse measured by recording the momentum of a trap bar in contact with the distal end of the main bar. By varying the length of the trap bar, Hopkinson was able to obtain records of the impulse contained in various durations of the stress wave. By repeated tests with nominally identical loading and different length trap bars, Hopkinson was able to contrast reasonable approximations of the cumulative impulse-time history, and hence estimate the pressure-time history of the loading pulse.

The modern version of the HPB uses perimeter-mounted strain gauges to record the time history of the stress pulse. The variant of the instrumented HPB developed by Kolsky to study the dynamic behaviour of material properties (the Split-Hopkinson Pressure Bar, or Kolsky Bar [2]) is widely used. However, despite its relevance to the problem addressed here, relatively little work has been conducted on using the HPB in its original sense as a robust, high-bandwidth, high-capacity pressure transducer. Lee et. al. [3] used the HPB to study loading from near-field underwater detonations, whilst Esparza [4, 5] and Edwards et. al. [6] had earlier used HPB to measure blast loading in free air at scaled distances $Z < 0.1 \text{ m/kg}^{1/3}$.

In an effort to address this, a research programme is being conducted in the UK by the University of Sheffield and Dstl, using an approach similar to that of Esparza, with an array of HPBs mounted through holes in a stiff horizontal target plate such that the impact faces of the HPBs are flush with the lower face of the plate. This Characterisation of Blast Loading (CoBL) facility was originally designed to measure loading from shallow buried charges, but has more recently been used to measure free-air blast loading, with charges suspended below the target plate. Full details of the CoBL facility are provided in [7] and [8] with the rig shown diagrammatically in Figure 1. The CoBL facility typically uses 17 HPBs, one set epicentrally and four set at 90 degree spacing at radial offsets of 25, 50, 75 and 100 mm. Typically explosive charge masses in the range 50-300 grammes have been used in the CoBL test.

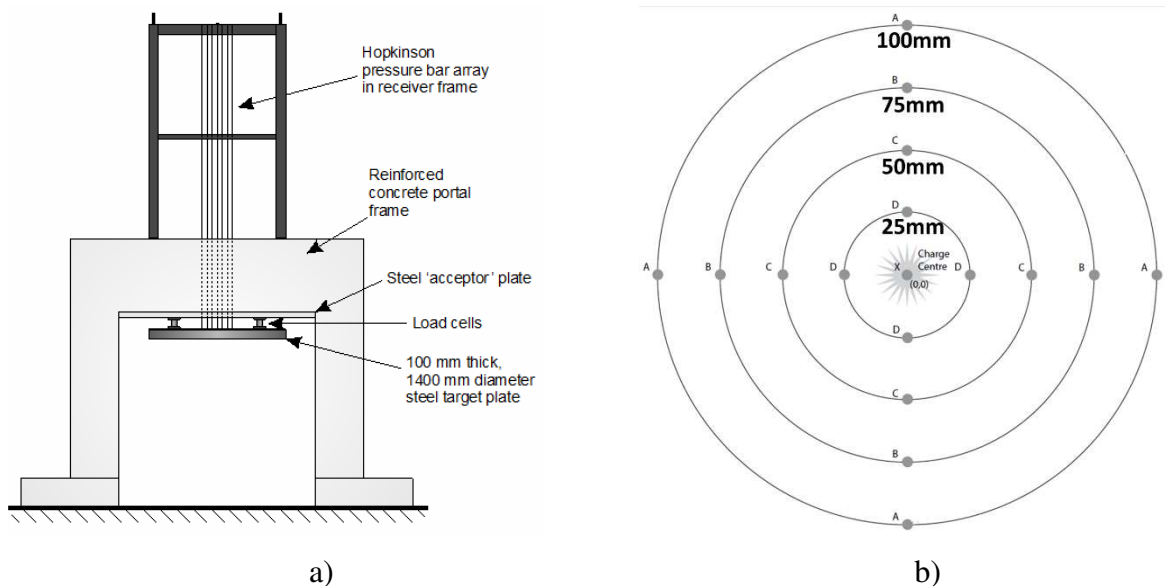


Figure 1. Schematic diagram of CoBL apparatus, a) front view and b) bottom view of plate and Hopkinson bar layout

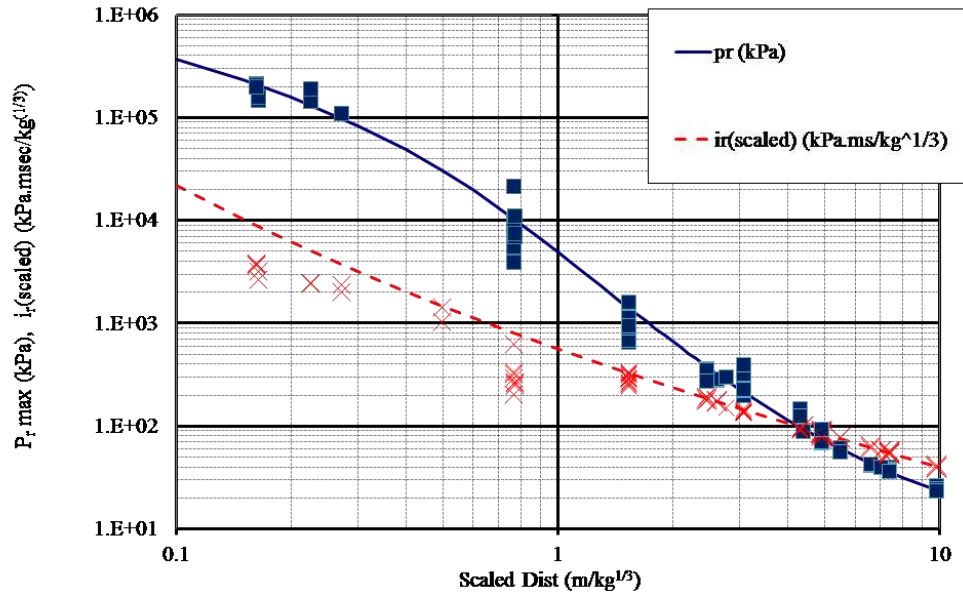


Figure 2. Comparison of experimental data and Kingery & Bulmesh predictions

Figure 2 shows a summary of CoBL data for normally reflected pressure and specific impulses from spherical PE4 and PE10 charges (scaled distance $<1 \text{ m/kg}^{1/3}$) together with reflected pressure and specific impulse data from far-field arena trials conducted at the University of Sheffield using conventional piezo-resistive pressure gauges mounted in a reflecting wall (scaled distance $>1 \text{ m/kg}^{1/3}$). The predictions from Kingery and Bulmesh [9] are also provided for comparison. Of note in these results is the fact that the experimental data in both the extreme near-field and the far-field are relatively consistent, whereas at intermediate scaled distances (around 0.5 to $2\text{-}3 \text{ m/kg}^{1/3}$) both the HPB and the piezo-resistive gauge data exhibit considerably more variability. This variability is believed to be due to Rayleigh-Taylor and Richtmyer-Meshkov instabilities in the fireball. In the extreme near-field, these instabilities have not had time to form, whereas in the far-field, irregularities in the shock front due to these instabilities have had time to equalize. However, at intermediate scaled distances, plumes of the fireball formed by these instabilities, or irregularities in the recently detached air-shock may, or may not strike the pressure sensors, resulting in large variations in loading. This is demonstrated in Figure 3, which shows the pressure-time histories from the epicentral CoBL HPB from two nominally identical tests, together with high speed video still images. In one test the HPB has been struck by an instability plume running ahead of the main fireball, whereas in the other, the HPB has been struck by the main fireball/air shock, resulting in large variations in arrival time and loading magnitude.

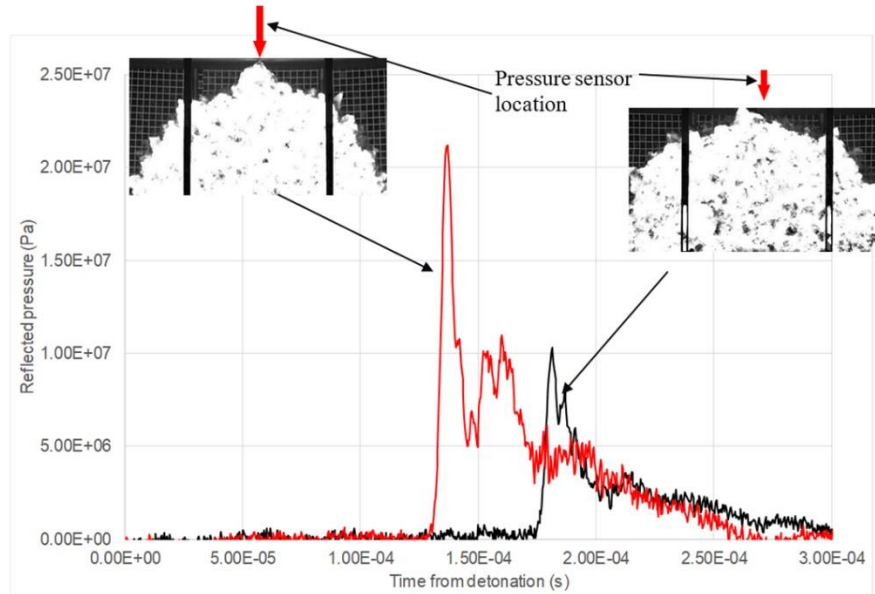


Figure 3. Variations in loading due to fireball instabilities – Scaled distance $0.76 \text{ m/kg}^{1/3}$, epicentral CoBL HPB

Prior to conducting the near-field tests, a series of small-scale open-air arena tests were conducted to assess the consistency of far-field blast waves produced by small PE4, PE8 and PE10 charges. These tests were all conducted using a 0.250 kg hemispherical explosive charge, placed on small steel anvils on top of a reinforced concrete ground slab. The normally reflected pressure was recorded at gauge station G1 in Figure 4, using a flush-mounted (to a steel plate) Kyowa KSP piezo-resistive pressure gauge located at the foot of a large reflecting wall surface (a 300 mm thick reinforced concrete bunker wall, faced with solid concrete blocks). The wall was of sufficient dimensions to render edge conditions irrelevant with respect to the duration of the blast loading. The small steel plates to which the gauges were mounted have now been replaced with larger plates to eliminate clearing effects on the pressure traces, see Figure 5. A more recent adaptation of this test setup also makes use of a sand-filled trench between the two parallel walls, which allows the hemisphere to be mounted flush with ground level and located at any distance between the walls.

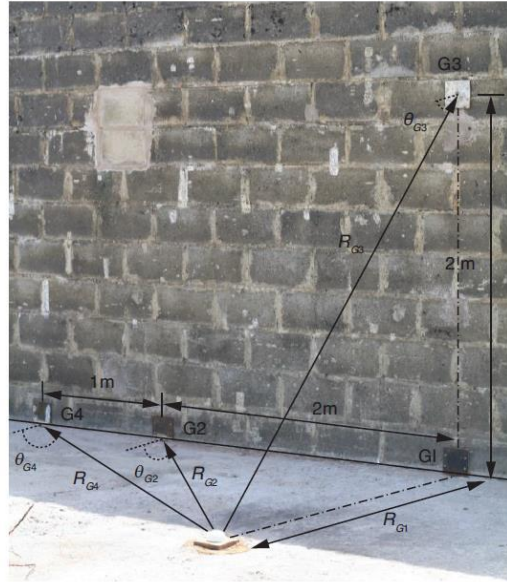


Figure 4. Set-up for far-field arena tests of hemispherical PE10 charges

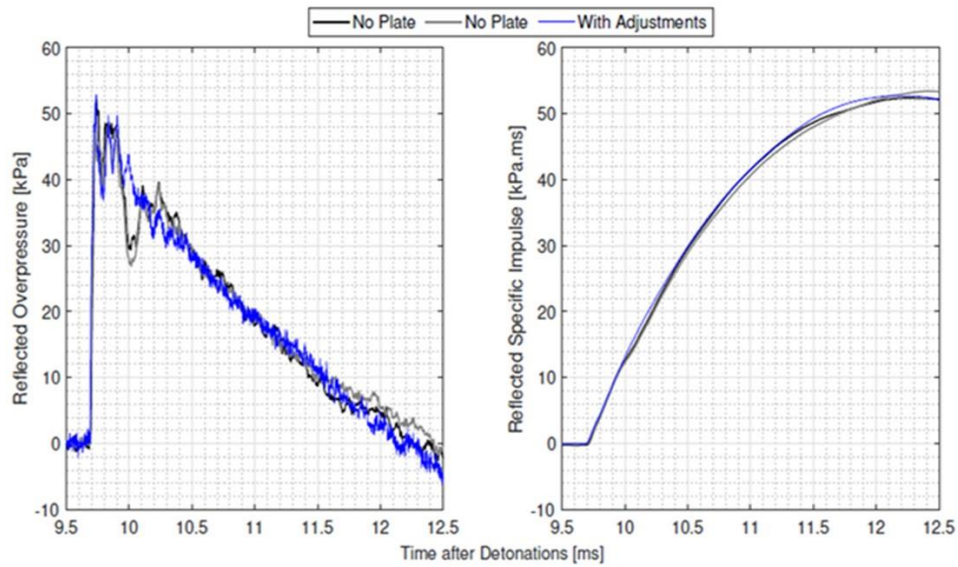


Figure 5. Comparison of pressure-time history with small (black) and large gauge plates (blue)

Confined testing has also been conducted at Blastech using a fully-sealed steel pipe, Figure 6, which can be filled with either air, nitrogen or argon. Pressure gauges are mounted within hollowed-out bolts to reduce thermal (or fragmentation) effects but allow accurate measurement of long-term QSP (Quasi-Static Pressure). Pyrometry can also be included to record measurements of fireball or gas temperature.

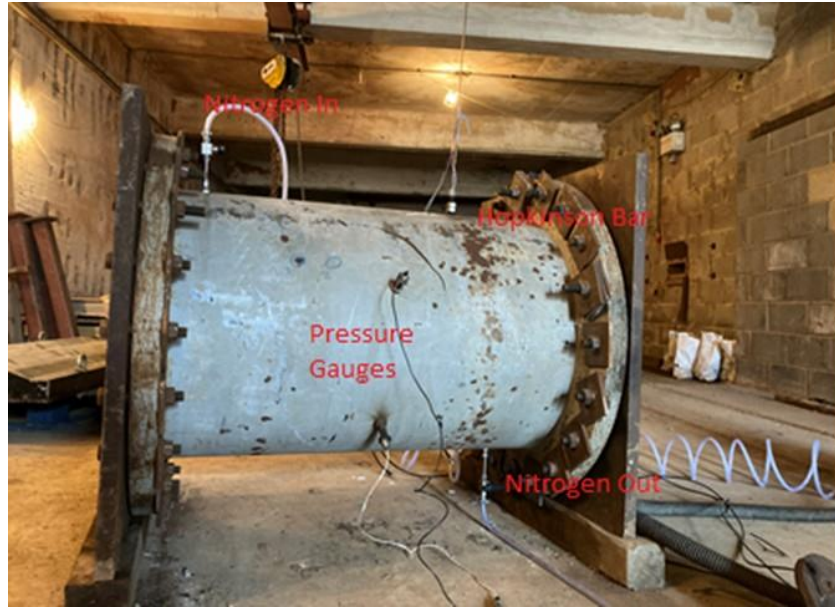


Figure 6. Set-up for confined tests of spherical plastic explosive charges

CYLEX tests, Figure 7, have also been conducted at Dstl, Porton Down on a series of energetic materials. HetV (Heterodyne Velocimetry) is used to measure the wall velocity of the cylinder expansion. Cylinders are typically 25 mm internal diameter x 300 mm long, accurately machined from high purity copper and containing approximately 150-250 g of energetic material.



Figure 7. Set-up for confined tests of spherical plastic explosive charges

DETERMINATION OF PARAMETERS USING THERMOCHEMICAL SOFTWARE

The numerical simulations in this paper (unless otherwise stated) were conducted using the APOLLO Blastsimulator CFD (Computational Fluid Dynamics) software [10, 11, 12], developed by Fraunhofer EMI, Germany. The APOLLO software solves the conservation equations for

transient flows of compressible, inviscid and non-heat conducting, chemically reacting fluid mixtures.

The fluid system considered for the analysis of blast effects consists of two components: the gaseous detonation products and the ambient air. The first is modelled with a JWL (Jones-Wilkins-Lee) EOS (Equation Of State), the latter is considered a thermally perfect gas. A quadratic polynomial function of the temperature is used as approximation for the caloric equation of state for each fluid. The detonation process is modelled on the basis of the Chapman-Jouguet theory. An empirical afterburn model is used to account for the effects of afterburning of oxygen-deficient explosives.

$$p = C_1 \left(1 - \frac{\omega \rho}{R_1 \rho_0}\right) e^{-R_1 \rho_0 / \rho} + C_2 \left(1 - \frac{\omega \rho}{R_2 \rho_0}\right) e^{-R_2 \rho_0 / \rho} + \rho R T$$

$$p = a_0^2 (\rho - \rho_0) + p_0$$

$$p = \rho R T$$

$$e = e_0 + c_{V1} T + c_{V2} T^2$$

For the numerical solution of the equations a finite volume scheme with explicit time integration is applied. The time integration is performed with a two-step scheme, which consists of a Lagrange step (acceleration and deformation of a material volume) and a subsequent step in which the updated material volume is remapped back onto the mesh cells. In the Lagrange step a characteristics-based, linearized calculation of pressure and velocity at cell interfaces is used; the remapping step is performed with the donor-cell method. These methods combine computational efficiency and flexibility, as they are not limited to specific types of equations of state. Local thermal equilibrium is assumed for finite volumes (grid cells) containing gas mixtures: all gases within a cell are supposed to be fully diffused and have the same temperature. The resulting pressure in a mixed cell thus is the sum of the partial pressures.

The finite volume method is extended to second order accuracy via a tri-linear reconstruction of the distribution of the conservative variables within the grid cells. Each linear reconstruction is controlled through a UMIST limiter, [13], the coefficients of which have been adjusted to ensure accuracy and robustness. In addition, the three originally independent spatial reconstructions have been coupled to achieve an improved spatial isotropy of the second order extension.

The simulations discussed in this paper made use of an afterburning model, Infinite Rate (IR), with the exception of the tests in Nitrogen where no afterburn was included. The IR model is based on a concept originally suggested in [14] by Alan Kuhl. It is based on the assumption that the combustion of the (oxygen-deficient) detonation products with the oxygen of the air is solely governed by the turbulent mixing of the reactants at the unstable surface of the fireball. Reaction times from kinetic energy are assumed to be negligible compared to the characteristic flow times as density and temperature are sufficiently high in the reaction zone. This is modelled numerically by the instantaneous combustion of the reactants in one grid cell within one time step in stoichiometric proportions. The combustion products are modelled as thermally perfect gases. The EOS parameters for all components (detonation products, combustion products and air) have been determined by fitting the respective EOS to data sets obtained with the thermochemical code Cheetah [15] or EXPLO5.

The methodology for developing the parameters for energetic materials was provided by Fraunhofer EMI and updated for use in Cheetah v7 and EXPLO5. All EOS used in this paper were developed using thermochemical software by either Fraunhofer EMI or Dstl.

NUMERICAL MODELLING

The APOLLO models were run using the Dynamic Mesh Adaption (DMA) functionality which dynamically refines and un-refines the mesh to create an accurate and efficient simulation. Mesh resolutions described here refer to the highest resolution level within each model (the maximum resolution that the model can refine to). Each model was run in three-dimensions (3D) using zoom stages, with each stage using a coarser resolution over a greater volume (i.e. stage 1 could use a 1 mm mesh for a distance of 100 mm from the charge centre, then stage 2 could use a 2 mm mesh for 200 mm from the charge centre). The reflecting surfaces were modelled as wall boundary conditions and ambient boundaries² were placed on the remaining sides of the model.

All far-field tests simulations were conducted using 90% of the charge mass to account for 10% energy loss to the ground, which is not captured by the simulations using a perfectly rigid boundary for the ground. This value was chosen based on the Conwep³ approach of spherical vs hemispherical predictions [16].

There is a known issue when predicting the early arrival time of the secondary shock⁴ [17] in APOLLO when IR afterburn is included, which is currently being rectified. This can also lead to an over-prediction in the peak specific impulse if the secondary shock arrives during the positive phase.

All EOS produced by Dstl have been used directly within APOLLO in the below studies, without refinement, calibration, modification or previous comparison to experimental data. A standard program burn (burn on time) [18] detonation model was used in all simulations.

1. VALIDATION STUDIES OF IDEAL PLASTIC EXPLOSIVES

Tests and modelling have been conducted for PE4, PE8 and PE10 for a range of charge masses and stand-off distances for near-field, far-field and confined tests discussed in this section. This process has established a robust and consistent method for thermochemical parameterisation and numerical modelling techniques for ideal plastic explosives, where a single set of EOS parameters can be used over a wide range of energetic regimes. A sample of this work is presented here and is representative of all the work undertaken.

Ambient boundaries are used to allow pressure and fluid to flow out through the boundary of a model. This² essentially allows a much smaller volume to be simulated, representing a semi-infinite volume of space
Conwep is a software code with a collection of conventional weapons effects calculations from the equations and³ curves of TM 5-855-1. It provides predictions of a wide range of effects including airblast, fragment penetration and ground shock. It is typically used as approximate validation of peak pressure and specific impulse predictions
When the detonation wave reaches the outer boundary of an explosive a rarefaction wave forms and travels back⁴ through the material. For a spherical explosive, this wave coalesces at the centre of the charge, causing large compression resulting in a secondary shock wave transmitted back through the material and out into the surrounding medium

EOS's were developed and compared using both thermochemical codes available to Dstl, Cheetah v7 and EXPLO5. The figures in the following sections use a label of Cheetah or EXPLO5 to display which EOS was used, however all models were simulated in APOLLO, unless otherwise stated.

A. FAR-FIELD TESTS

Far-field tests were conducted at Blastech using 250 g hemispherical ground burst charges. In APOLLO they were simulated in contact with a rigid boundary representing the floor, the wall was also represented by a rigid boundary and a rigid plate was placed on the wall representing the gauge mounting plate. The models were run in half symmetry, including IR afterburn, using 5 stages with the following setup:

- Stage 1 – 0.78 mm resolution for a distance of 100 mm from the charge centre
- Stage 2 – 1.56 mm resolution for a distance of 200 mm from the charge centre
- Stage 3 – 3.125 mm resolution for a distance of 1.2 m from the charge centre
- Stage 4 – 6.25 mm resolution for a distance of 2.2 m from the charge centre for the 2 m stand-off and 8.2 m for the 8 m stand-off (recording the peak pressure)
- Stage 5 – 12.5 mm resolution for the remainder of the model

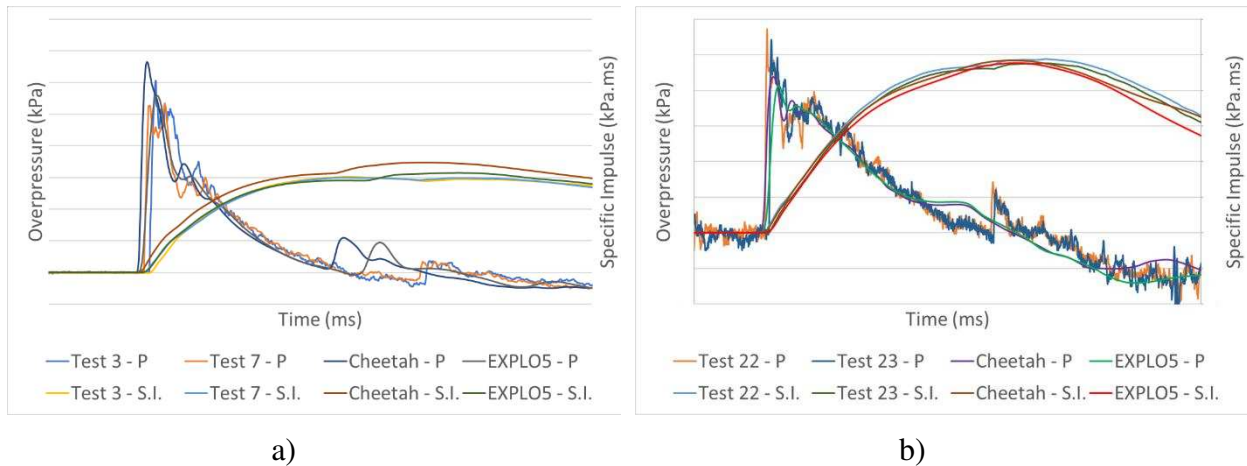


Figure 8. Normally reflected pressure and specific impulse vs time from free-air arena tests for a) PE8 at 2 m and b) PE10 at 8 m. Comparison of experimental and numerical model results

B. NEAR-FIELD TESTS

Near-field tests were conducted at Blastech using approximately 200 g spherical charges of PE10 at a stand-off distance of 125 mm. In APOLLO they were simulated with the COBL plate represented by a rigid boundary and gauges placed at the location of each HPB. The models were run in quarter symmetry, including IR afterburn, using two stages with the following setup:

- Stage 1 – 0.5 mm resolution for a distance of 32 mm from the charge centre
- Stage 2 – 1 mm resolution for the remainder of the model

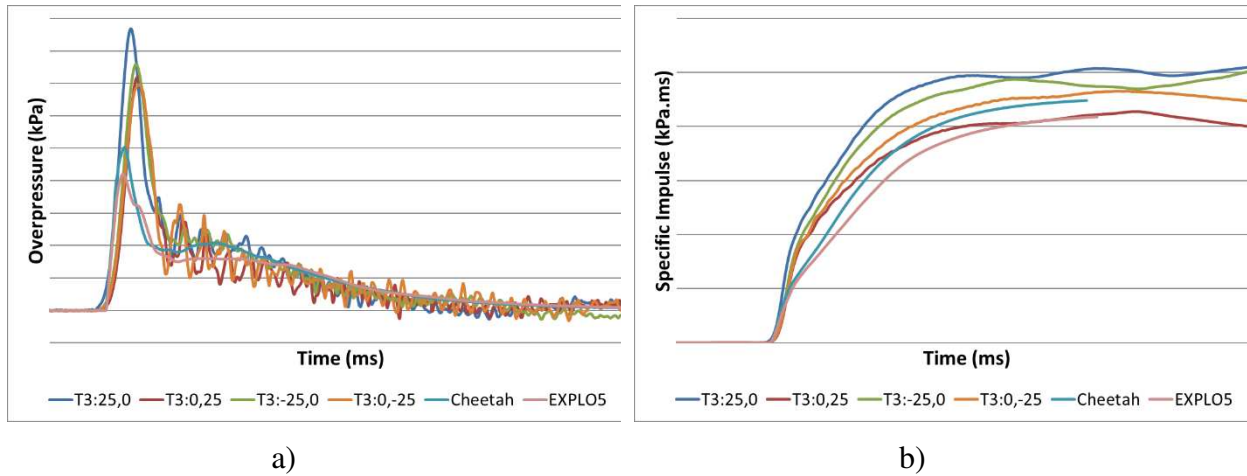


Figure 9. a) Reflected pressure vs time and b) reflected specific impulse vs time from COBL tests for approximately 200 g of PE10 at 125 mm (25 mm lateral position). Comparison of experimental and numerical model results

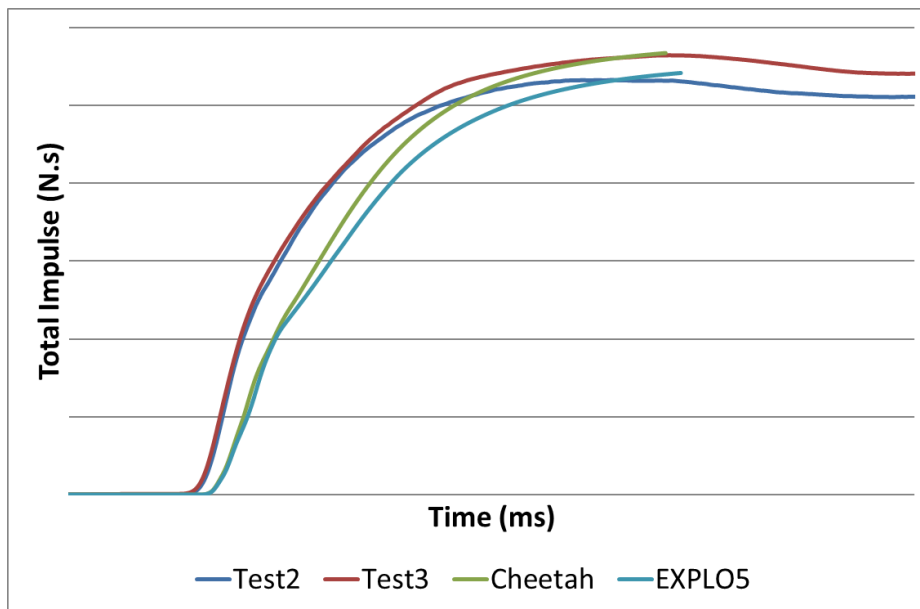


Figure 10. Reflected total impulse vs time from COBL tests for approximately 200 g of PE10 at 125 mm. Comparison of experimental and numerical model results

C. CONFINED TESTS

Confined tests were conducted at Blastech using 30 g PE8 spherical charges in both air and nitrogen. In APOLLO they were simulated in the centre of the chamber, 270 mm from one end and the chamber was represented by a rigid cylinder, the gauge was placed on the inside of the chamber wall (the hollowed out bolt containing the gauge was not modelled). The models were run in quarter symmetry, including IR afterburn, using 6 stages with the following setup:

- Stage 1 – 0.195 mm resolution for a distance of 25 mm from the charge centre
- Stage 2 – 0.391 mm resolution for a distance of 50 mm from the charge centre
- Stage 3 – 0.781 mm resolution for a distance of 100 mm from the charge centre
- Stage 4 – 1.56 mm resolution for a distance of 200 mm from the charge centre
- Stage 5 – 3.125 mm resolution for a distance of 450 mm from the charge centre
- Stage 6 – 6.25 mm resolution for the remainder of the model

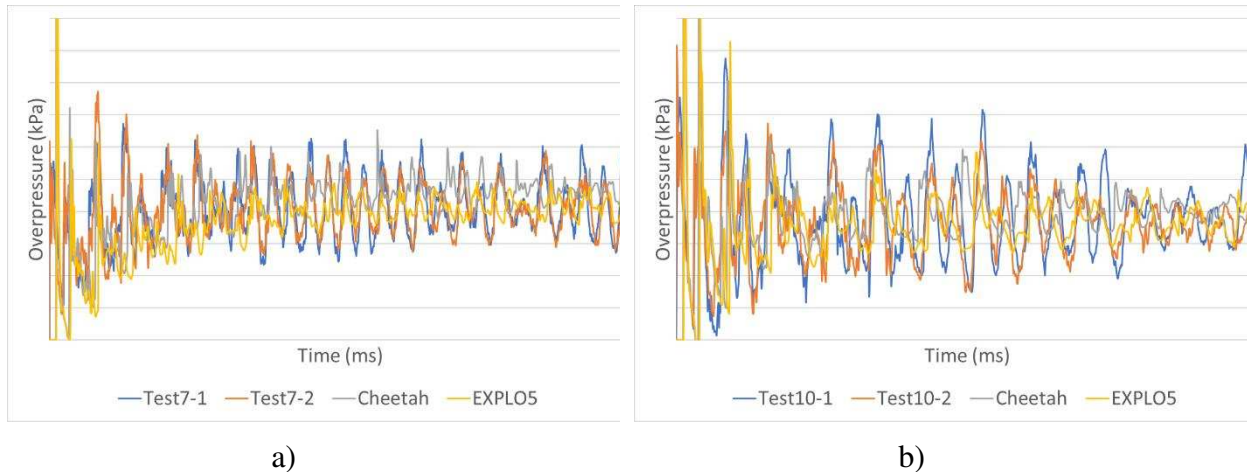


Figure 11. QSP vs time from fully confined test of 30 g of PE8 in a) air and b) nitrogen. Comparison of experimental and numerical model results

D. CYLEX TESTS

Confined tests were conducted at Dstl using ideal plastic explosive. The tests were simulated in Autodyn (due to the lack of suitable copper EOS in APOLLO) using a shock EOS for the copper cylinder. The model used 2D axial symmetry and represented all materials using an Eulerian mesh. The wall velocity was measured using a Lagrangian gauge which flowed with the fluid in the model. Figure 15 below shows the results of four simulations:

- A CTH⁵ model where the JWL parameters were calibrated to match the wall velocity curve from the test
- An Autodyn⁶ model using a uniform 0.1 mm resolution, with the JWL parameters calibrated in CTH
- An Autodyn model using a uniform 0.2 mm resolution, with the JWL parameters determined from Cheetah v7

CTH is an export-controlled Eulerian code developed by SANDIA, US. The software has a range of functionality⁵ and is primarily used by Dstl for metal pushing applications and detailed detonation simulation. Autodyn is a commercial versatile FV (Finite Volume) code developed by ANSYS, US. The software has a very⁶ wide range of functionality, including Euler, Lagrange and SPH (Smoothed Particle Hydrodynamics) integration schemes, and is used across many sectors

- An Autodyn model using a uniform 0.2 mm resolution, with the JWL parameters determined from EXPLO5

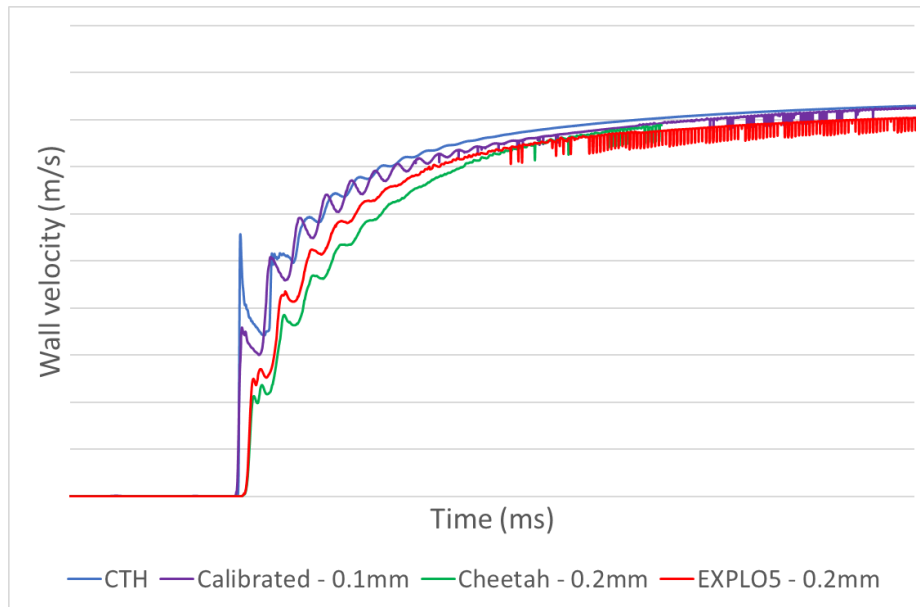


Figure 12. Wall velocity vs time from CYLEX test of plastic explosive. Comparison of CTH calibrated JWL and numerical model results

2. NON-IDEAL ENERGETIC TESTS

The previous section showed the methodology for parameterising and simulating ideal explosive behaviour has been established. It was then of interest as to how these methods can be transitioned for various non-ideal explosives, including mixed fuel-oxidisers (e.g. ANFO), porous materials or aluminised charges.

A. FAR-FIELD SMALL-SCALE ANFO TESTS

ANFO is a very non-ideal material, the behaviour of which exhibits a large dependence on its explosive mass, where “ideal” ANFO behaviour is not experienced until in the range of 100 kg+. Therefore, 250 g hemispherical charges were detonated (from the top and bottom) in the far-field test setup. Excellent consistency was observed in repeat tests, even when varying the detonation position from top to bottom, except for a 1 m stand-off. In this case a significant difference can be seen in the pressure time history between the top and bottom detonated charges, Figure 13a). The large difference between “ideal” ANFO, represented by Conwep predictions, and small-scale ANFO can be seen in Figure 13.

It was determined to attempt to simulate the minimal output of the ANFO charges, to bound the problem. Therefore, EXPLO5 was used to determine an EOS for AN and in the APOLLO simulation the mass of the fuel oil was also ignored. This was then simulated using a program burn detonation model with a constant detonation velocity, taken as the average measured from the tests. These simulations produced very representative predictions of the small-scale far-field behaviour including the effect of detonator position.

Due to this positive result, various investigations are ongoing to attempt to capture the scaling behaviour of ANFO with charge mass. This includes explicitly modelling the ANFO prills and porosity, using the porosity method discussed in the next section, along with afterburning of the fuel oil and a program burn model with a non-constant detonation velocity.

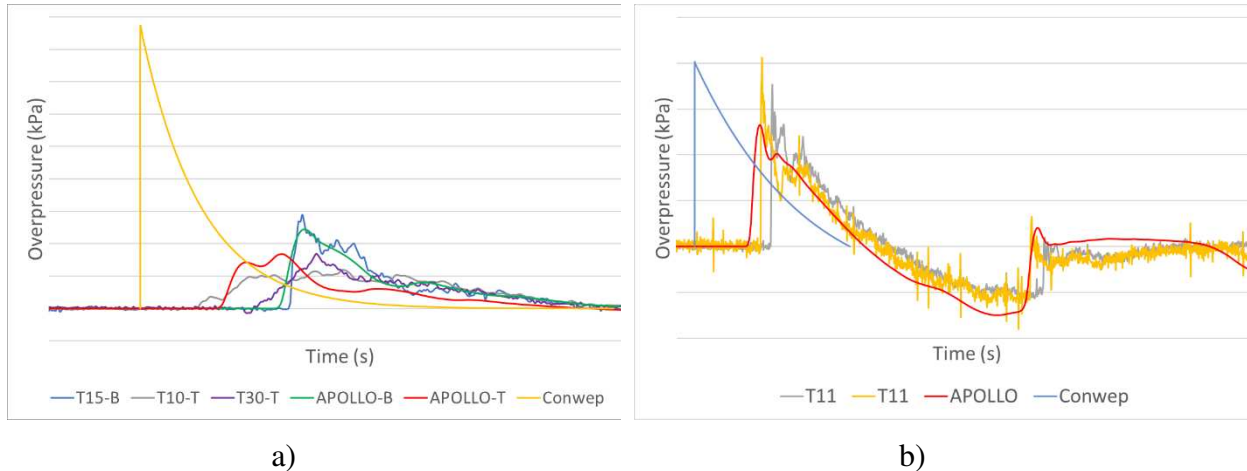


Figure 13. Reflected pressure vs time from far-field small-scale ANFO tests at a) 1m and b) 5m. Comparison of test, Conwep and numerical model results

B. POROUS IDEAL ENERGETIC MATERIAL

Free-field tests were conducted by CEA, France, on five ideal energetic materials in a very porous, powdered form, with a bulk density approximately 40-60% of their standard density. Incident pressure measurements were taken at a range of scaled distances between approximately $1.25-6.3 \text{ m/kg}^{1/3}$. These tests were initially simulated using two methods, as shown in Figures 18-21.

- Method A – Default EOS using standard density (correct mass but much smaller charge geometry than in the tests) – detonation velocity lowered to that from EXPLO5 for porous density
- Method B – EXPLO5 EOS using porous density

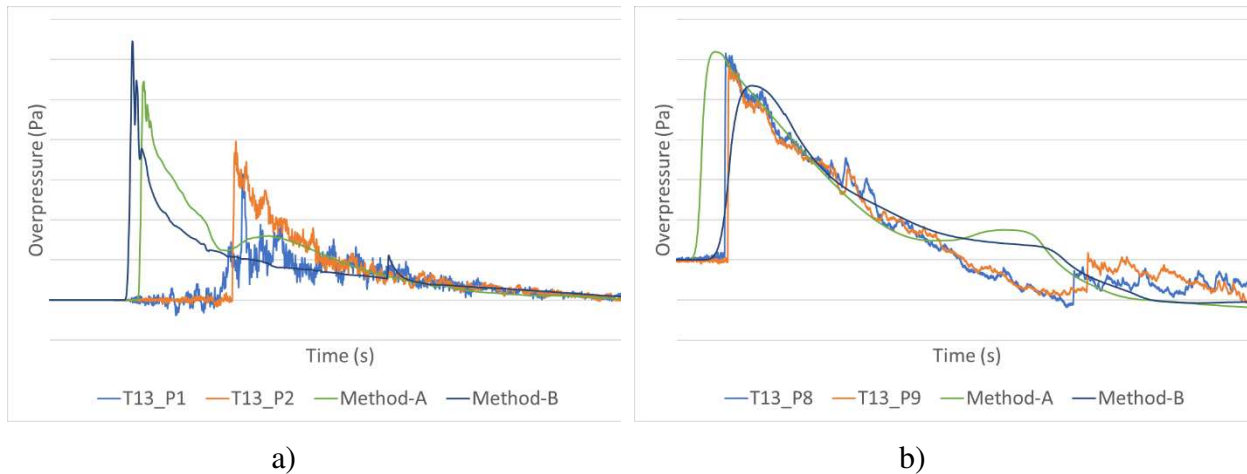


Figure 14. Incident pressure vs time from a free-field test of material 2 at a) closest stand-off and b) furthest stand-off. Comparison of experimental and numerical model results

A mixture of results were obtained, where for material 1 the predictions were very reasonable for both the closest and furthest gauges, for both pressure and specific impulse. However, the results for the other four materials were much worse, with material 2 showing extremely poor predictions at the closest gauge, Figure 14.

It was therefore requested that functionality was developed by Fraunhofer EMI to allow porosity to be explicitly captured within the charge description in APOLLO. This method allowed elements filled with air to be inserted into the charge geometry, Figure 15, using the standard EOS⁷ for the energetic material at its typical bulk density. A program burn model was used, with the detonation velocity calculated from EXPLO5 for the porous density, and IR afterburn was also included within the detonation.

The porosity was selected to create the correct bulk density used in each test. The pressure and specific impulse predictions for the closest and furthest gauges are shown below in Figure 17 to Figure 20, for material 1 and material 2 (where the results are representative of all five materials). Excellent correlation is seen for all materials from relatively near-field to far-field distances, showing that this technique can be used to obtain accurate predictions without the need to generate density specific EOS.

The EOS for four materials available within the APOLLO library were used. The EOS for the fifth material was⁷ calculated using EXPLO5 using the technique established for the ideal plastic explosives

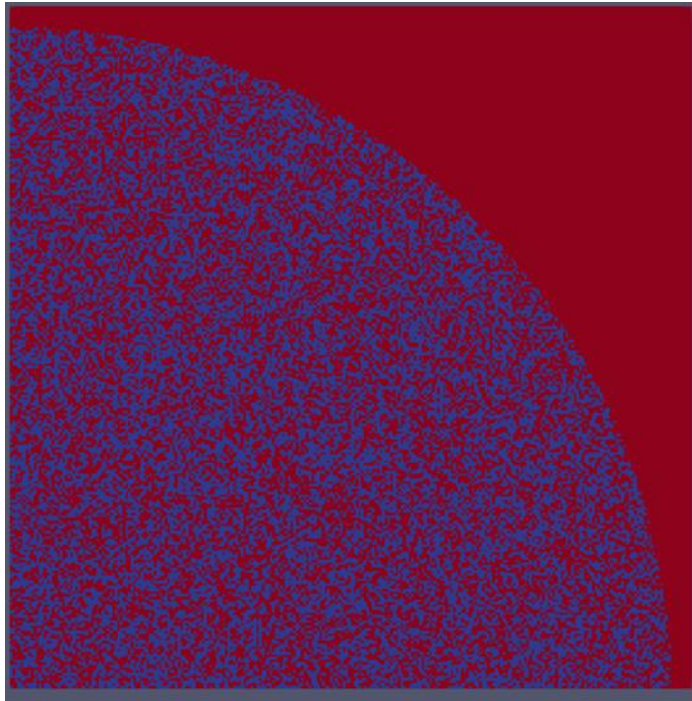


Figure 15. Charge geometry for material 1, with air (red) pores included

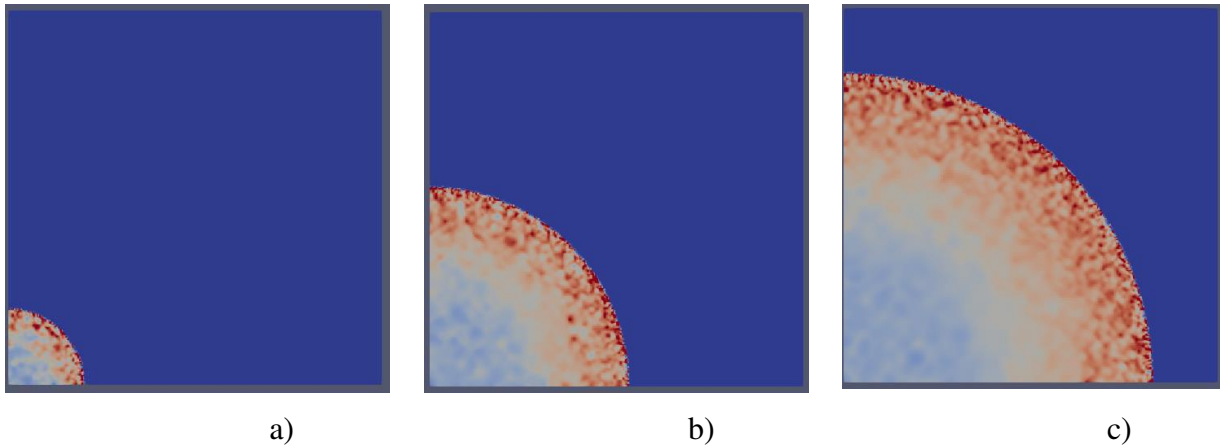


Figure 16. Expansion of pressure through the charge geometry during detonation, for material 1

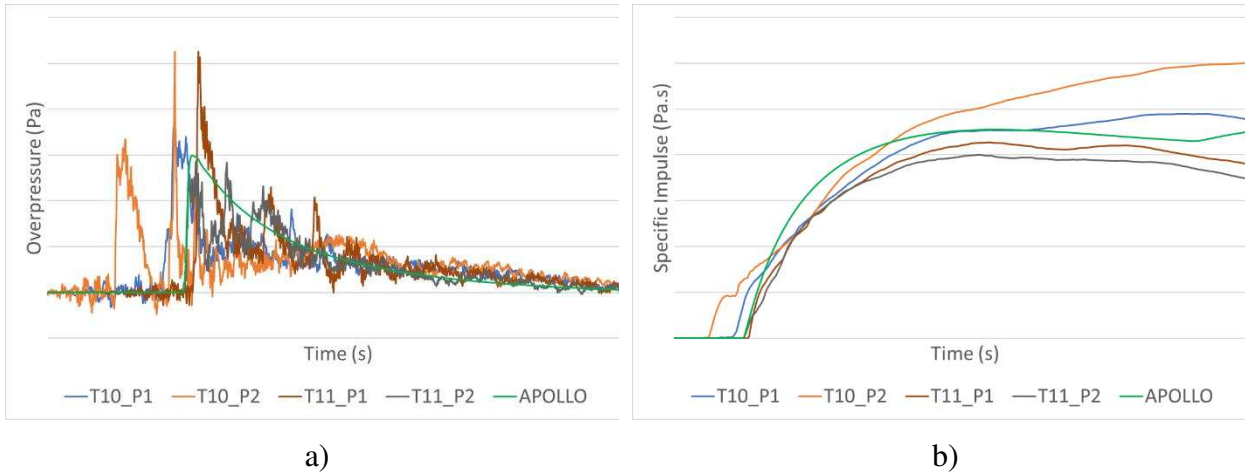


Figure 17. a) Incident pressure vs time b) and specific impulse vs time from a free-field test of material 1 at closest stand-off. Comparison of experimental and numerical model results

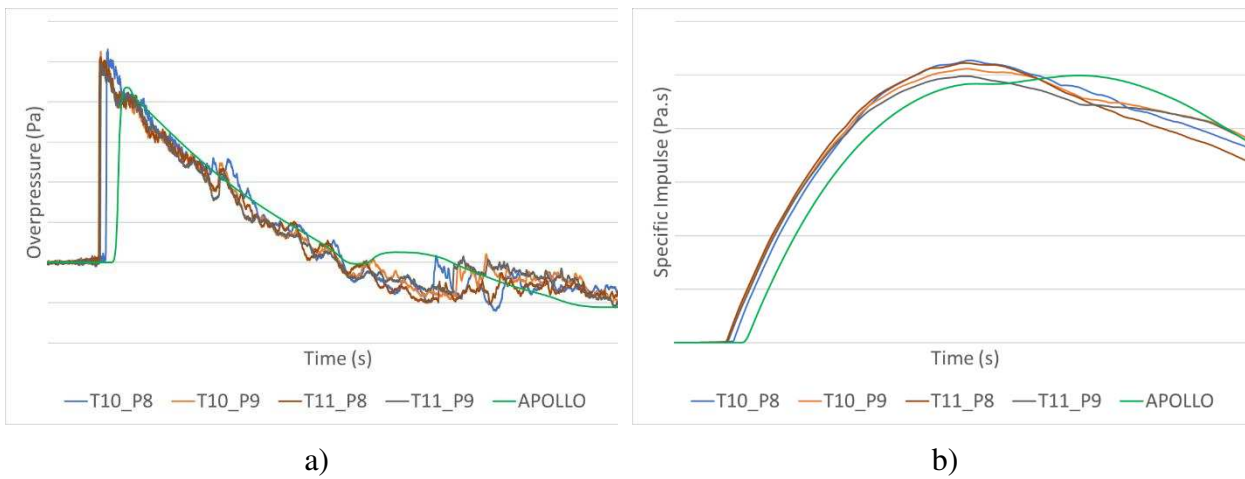


Figure 18. a) Incident pressure vs time b) and specific impulse vs time from a free-field test of material 1 at furthest stand-off. Comparison of experimental and numerical model results

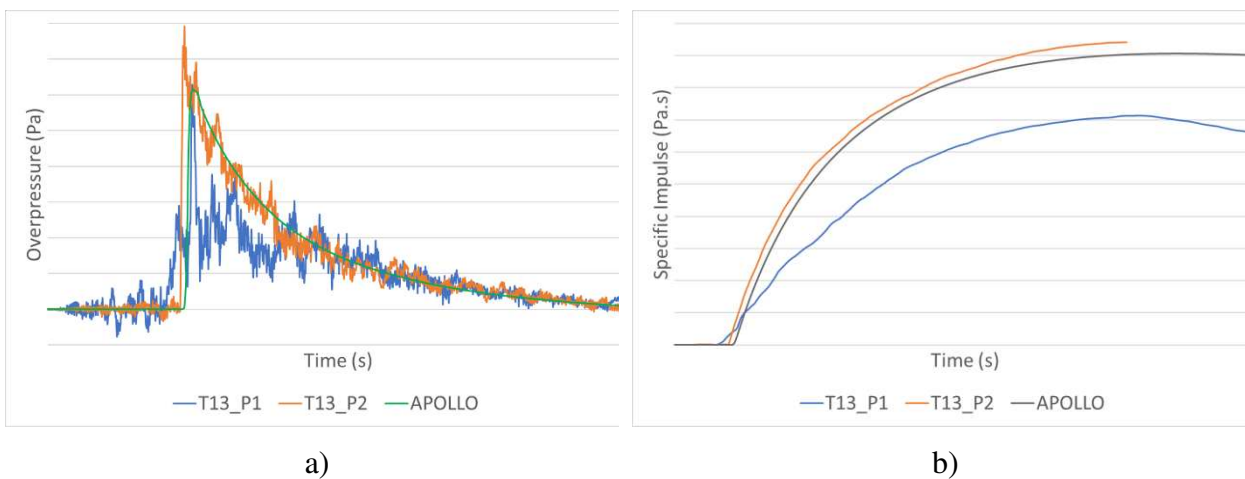


Figure 19. a) Incident pressure vs time b) and specific impulse vs time from a free-field test of material 2 at closest stand-off. Comparison of experimental and numerical model results

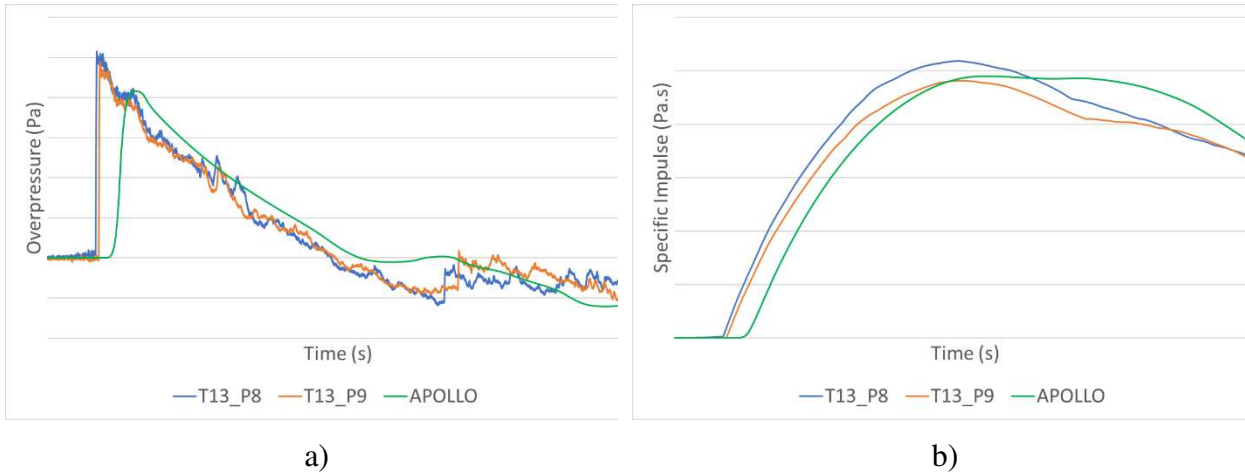


Figure 20. a) Incident pressure vs time b) and specific impulse vs time from a free-field test of material 2 at furthest stand-off. Comparison of experimental and numerical model results

A resolution study⁸ was then also conducted for material 2, where the detonation of the explosive was performed with four different resolutions, 1 mm, 500 μ m, 200 μ m and 100 μ m. This was then remapped into an identical model and run until completion. The results below in Figure 21 show that there is very little sensitivity to the resolution and that simply including the porosity in the charge was required to obtain representative predictions.

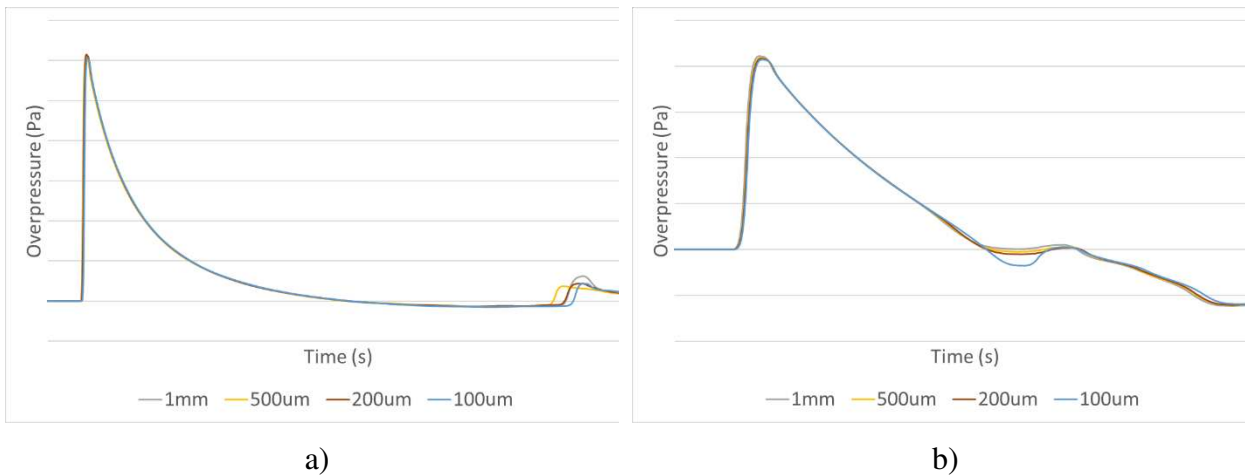


Figure 21. Incident pressure vs time at a) closest gauge and b) furthest gauge for material 2

Numerical simulations, especially when predicting peak pressure values, are very sensitive to the mesh resolution used. Therefore, resolution studies are conducted in order to determine suitable mesh resolution, where convergence is achieved, or to understand the level of under-prediction of the used resolution if convergence resolution is not obtainable⁸

C. ALUMINISED EXPLOSIVES

As mentioned in the introduction, tests have been performed on PBXN-109 charges in near-field, far-field and confined configurations. To date, only the results from the far-field and confined tests have been processed and analysed. The charges were manufactured with 64% RDX, 20% aluminium and 16% binder, into 250 g hemispheres for the far-field tests and 20 g and 50 g spheres for the confined tests.

An initial material model was developed by Fraunhofer EMI (before access to any test data) including the EOS for the energetic material (without aluminium), aluminium, reactions and metallic products. This material model was then included in initial simulations by Dstl using Lagrangian reactive particles for the aluminium, of both the far-field and confined tests, which can be seen in Figure 22 to Figure 24 below.

The far-field results produced an excellent prediction of arrival time, peak pressure and specific impulse at both 3 m and 8 m stand-off distances. The confined tests were simulated in both air and nitrogen (where simulations were conducted with inert aluminium particles). The results in both atmospheres showed very good agreement with the test data until the pressure decay caused by thermal losses kicked in.

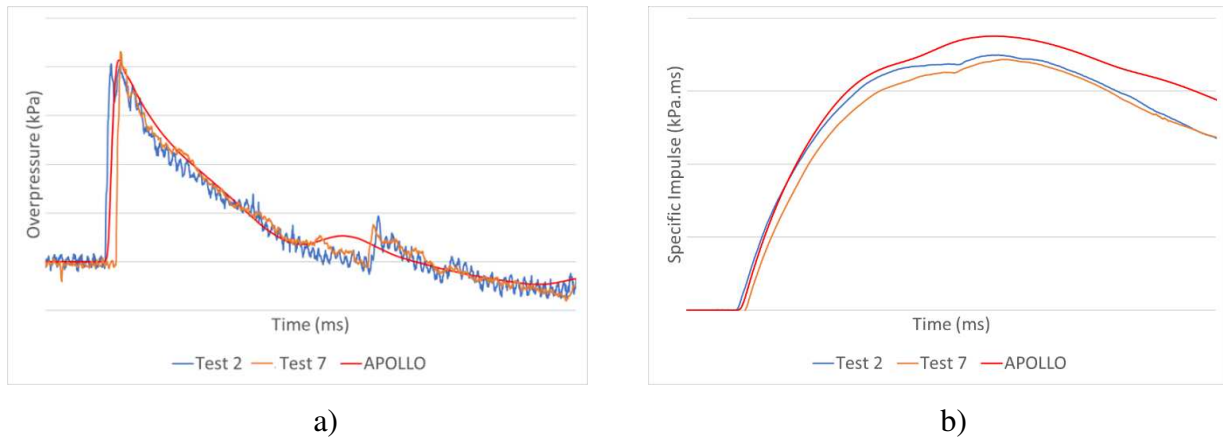


Figure 22. Normally reflected a) pressure and b) specific impulse vs time from free-air arena tests for PBXN-109 at 3 m. Comparison of experimental and numerical model results

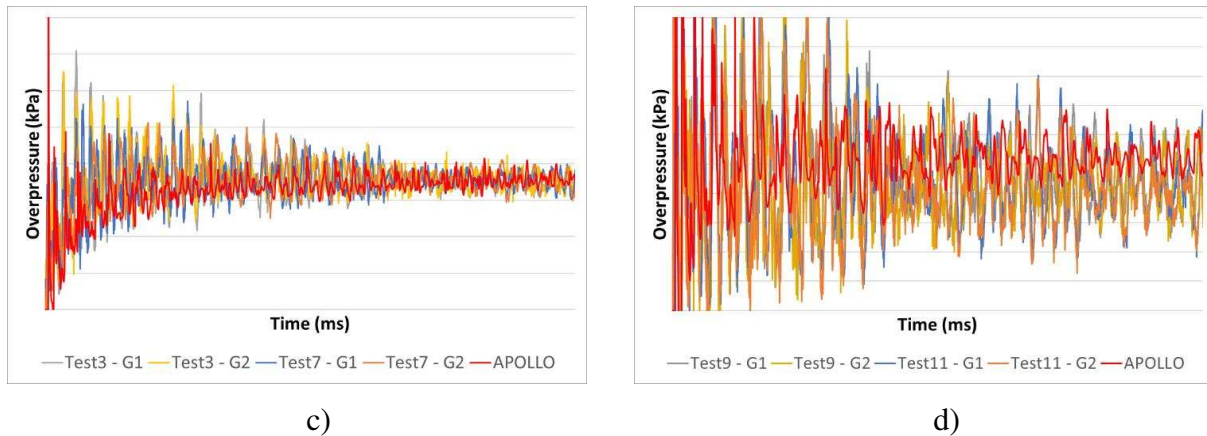


Figure 23. QSP vs time from fully confined test of 20 g of PBXN-109 in a) air and b) nitrogen. Comparison of experimental and numerical model results

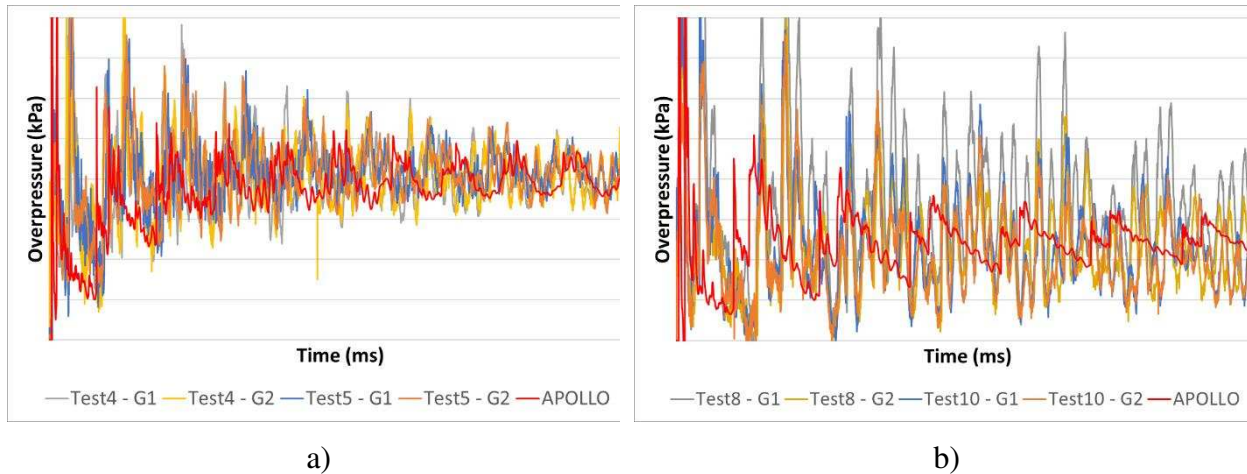


Figure 24. QSP vs time from fully confined test of 50 g of PBXN-109 in a) air and b) nitrogen. Comparison of experimental and numerical model results

CONCLUSIONS

A series of well controlled, highly instrumented tests has been established and conducted across a range of regimes on numerous ideal and non-ideal explosive materials. It has been shown that for ideal plastic explosives a single EOS can be developed from thermochemical codes that when implemented into APOLLO provides accurate predictions across a range of regimes from CYLEX, near-field, far-field and confined, including explicit afterburn. These EOS can also be used for ideal porous materials if the porosity is explicitly included within the model, with only a reduction of detonation velocity required to produce representative results.

For non-ideal materials such as ANFO, the complex detonation makes the predictions far more challenging. However, it can be seen that bespoke EOS can be developed, using thermochemical codes, to match experimental data, although without additional functionality these EOS will not produce the scaling experienced by these charges. Additional investigations are ongoing to determine if relatively simple functionality can be included to allow scaled results to be determined.

For aluminised explosives, it has been shown that when explicitly including the aluminium particles as reactive Lagrangian particles within a model, accurate results can be predicted for a range of regimes. The work is currently only at its preliminary stage but the initial results for far-field and confined tests appear very promising and this method will be used for a wider range of tests, including near-field, and materials, including PBXN-111.

Acknowledgements: Fraunhofer EMI, AFRL and CEA

REFERENCES

- [1] B. Hopkinson, "Method of Measuring the Pressure Produced in the Detonation of High Explosives or by the Impact of Bullets," *Philosophical Transactions of the Royal Society of London. Series A*, vol. 213, p. 437–456, 1914.
- [2] H. Kolsky, "An Investigation of the Mechanical Properties of Materials at Very High Rates of Loading," *Proceedings of the Physical Society. Section B*, vol. 62, no. 11, p. 676, 1949.
- [3] C. Lee, R. C. Crawford, K. A. Mann, P. Coleman and C. Petersen, "Evidence of higher Pochhammer-Chree modes in an unsplit Hopkinson bar," *Measurement Science and Technology*, vol. 6, no. 7, pp. 853-859, 1995.
- [4] E. Esparza, "Blast measurements and equivalency for spherical charges at small scaled distances," *International Journal of Impact Engineering*, vol. 4, no. 1, pp. 23-40, 1986.
- [5] E. Esparza, "Reflected blast measurements near pancake charges," in *Proceedings of the 24th DoD Explosives Safety Seminar*, St Louis (MO), 1990.
- [6] D. H. Edwards, G. O. Thomas, A. Milne, G. Hooper and D. Tasker, "Blast wave measurements close to explosive charges," *Shock Waves*, vol. 2, p. 237–243, 1992.
- [7] S. D. Clarke, S. D. Fay, J. A. Warren, A. Tyas, S. E. Rigby and I. Elgy, "A large scale experimental approach to the measurement of spatially and temporally localised," *Measurement Science and Technology*, vol. 26, 2015.
- [8] A. Tyas, J. J. Reay, S. D. Fay, S. D. Clarke, S. E. Rigby, J. A. Warren and D. J. Pope, "Experimental Studies of the Effect of Rapid Afterburn on Shock Development of Near-Field Explosions," in *MABS24*, Halifax, NS, Canada, 2016.
- [9] C. N. Kingery and G. Bulmash, "Airblast parameters from TNT spherical air burst and hemispherical surface burst. Rep. No. ARBRL-TR-02555," U.S. Army Ballistic Research Laboratories, Aberdeen Proving Ground, MD, 1984.
- [10] A. Klomfass, A. Stoltz and S. Hiermaier, "Improved Explosion Consequence Modelling with combined CFD and Damage Models," *Chemical Engineering Transactions*, vol. 48, 2016.
- [11] A. Klomfass, T. Zweigle and K. Fischer, "A new AMR/ALE-solver for efficient simulation of detonations and blast waves," in *Proceedings of MABS 22*, Bourges, France, 2012.
- [12] [Online]. Available: <http://www.emi.fraunhofer.de/en/service-offers/software-solutions/apollo.html>.
- [13] F. S. Lien and M. A. Leschziner, "Upstream monotonic interpolation for scalar transport with application to complex turbulent flows," *International Journal of Numerical Methods in Fluids*, vol. 19, no. 6, p. 527–548, 994.
- [14] M. W. Howard, L. E. Fried and A. L. Kuhl, "Thermodynamic Model of Afterburning in Explosions," in *34th International ICT Conference: Energetic Materials: Reactions of Propellants, Explosives and Pyrotechnics*, Karlsruhe, Germany, 2003.
- [15] L. E. Fried, M. W. Howard and P. C. Souers, "CHEETAH 2.0 Users Manual, UCRL-MA-117541 Rev. 5," 1998.
- [16] U.S. Army Engineer Research & Development Center

- [17] Whittaker et al., “Evaluation of critical energetics modelling: Part 1 Explosives”, Dstl/TR134741, September 2021
- [18] Klomfass, Arno. 2020. “APOLLO Blastsimulator manual, Version 2020.2.”